



1 **Distinct Phototrophic Community Structure on a**
2 **Central Asian Glacier: Predominance of Filamentous**
3 **Cyanobacteria and Absence of Glacier Algae**
4 **(*Ancylonema* spp.)**

5 Yunjie Chen^{1,2}, Nozomu Takeuchi^{3*}, Sota Tanaka³, Saifei Li¹, Weizhen Zhang¹,
6 Xingyu Huang⁴, and Zhongqin Li⁵

7 ¹Center for Pan-Third Pole Environment, Lanzhou University, Lanzhou, China

8 ²Chayu Integrated Observation and Research Station of the Xizang Autonomous Region, Xizang,
9 China

10 ³Center for Environmental Remote Sensing, Chiba University, Chiba, Japan

11 ⁴Institute of Tibetan Plateau Research, Chinese Academy of Sciences, Beijing, China

12 ⁵State Key Laboratory of Cryospheric Sciences/Tien Shan Glaciological Station, Northwest Institute of
13 Eco-Environment and Resources, Chinese Academy of Sciences, Lanzhou, China

14 *Correspondence to:* Nozomu Takeuchi (ntakeuch@faculty.chiba-u.jp)

15 **Abstract.** Cold-adapted algae and cyanobacteria are key drivers of snow and ice albedo reduction, yet
16 their dynamics on dust-rich Central Asian glaciers remain poorly understood compared to the
17 well-documented algal blooms in the Arctic. This study investigated the spatio-temporal distribution of
18 phototrophic communities on Urumqi Glacier No.1, eastern Tien Shan, during a two-month melt
19 season. Our findings reveal a distinct seasonal succession where snow-covered surfaces were
20 dominated by snow algae *Chloromonadina* species (Chlorophyceae), while the exposure of bare ice
21 led to a sharp increase in biomass dominated by filamentous cyanobacteria (Oscillatoriaceae). Notably,
22 glacier algae such as *Ancylonema* spp., which drive darkening on Arctic ice, were entirely absent,
23 suggesting a fundamental ecological divergence. Statistical analyses indicated that cyanobacterial
24 proliferation is closely linked to environmental factors, showing significant positive correlations with
25 mineral-derived ions and negative correlations with inorganic nitrogen. These results, supported by
26 recent evidence that specialized cyanobacterial taxa drive the initiation and structural development of
27 cryoconite granules, suggest that high mineral dust deposition from surrounding arid regions facilitates
28 a stable, nutrient-limited niche for cyanobacteria. This "cyanobacteria-mineral synergy" creates a more
29 persistent biological darkening effect than the ephemeral algal blooms observed in polar regions. Our
30 study highlights the necessity of integrating region-specific microbial dynamics, which is characterized
31 by the absence of glacier algae and the dominance of mineral-buffered cyanobacterial communities,



32 into glacier mass balance models to improve the accuracy of future projections for Central Asian water
33 resources.

34 **1 Introduction**

35 Glacier and ice sheet surfaces constitute a distinct microbe-dominated biome within the Earth system
36 (Anesio and Laybourn-Parry, 2012), harboring an estimated 10^{29} microbial cells (Irvine-Fynn and
37 Edwards, 2014). The presence of liquid water, which is primarily from surface meltwater during the
38 summer melt season, is one of key limiting factors for microbial activity (Hodson et al., 2008).
39 Seasonal melting transforms glacier surfaces from a snow-covered landscape in winter to a mosaic of
40 habitats in summer, with bare ice prevailing in the ablation zones and snowpack persisting in
41 high-elevation accumulation zones (Stibal et al., 2012a). These snow and bare-ice habitats differ
42 markedly in their physical and chemical properties, leading to distinct microbial communities
43 (Yoshimura et al., 1997; Lutz et al., 2017). However, due to accelerated global glacier shrinkage
44 (Hugonnet et al., 2021), the spatial extent of microbial habitats on glacier and ice sheet surfaces is
45 rapidly diminishing. Therefore, investigating the spatial distribution and abundance of microbial taxa
46 across icy environment is not only critical for understanding the ecological dynamics of glacier surface
47 communities, but also for preserving a biological signature of these unique and increasingly vulnerable
48 ecosystems.

49 Algae and cyanobacteria are key cold-adapted photosynthetic microorganisms that play a dominant
50 role on biological carbon accumulation on glacier surfaces during melt season (Anesio et al., 2017).
51 For example, eukaryotic green algae contribute up to 97% of the total photoautotrophic carbon fixation
52 on the surface of the Midre Lovénbreen Glacier in Svalbard (Yallop et al., 2012). Cyanobacteria are the
53 primary contributors to photosynthetic activity, accounting for approximately 75%–93% of carbon
54 fixation within the cryoconite hole on Arctic glaciers (Stibal and Tranter, 2007).

55 In addition to their role in carbon cycling, these microorganisms contribute to the acceleration of
56 snow and ice melt by reducing surface albedo. Pigmented algae, can proliferate during the melt season,
57 leading to visible algal blooms that darken the surface of snow and ice and enhance solar radiation
58 absorption (Williamson et al., 2018; Takeuchi, 2013). Filamentous cyanobacteria produce extracellular
59 polymeric substances (EPS) that facilitate the aggregation of mineral particles, forming dark-colored



60 cryoconite granules (Stibal et al., 2012b; Yallop et al., 2012; Musilova et al., 2016), which further
61 lower surface albedo and enhance localized melting on glacier surfaces (Cook et al., 2016; Kohshima et
62 al., 1993; Takeuchi et al., 2018).

63 The habitats of algae and cyanobacteria on glacier surfaces are heterogeneous. In cryoconite and
64 cryoconite holes on ablation surfaces, filamentous cyanobacteria, particularly members of the order
65 Oscillatoriales, such as *Phormidesmis priestleyi*, *Phormidium* sp., and *Leptolyngbya* sp., are typically
66 dominant and play a crucial role in formation of cryoconite granules (Singh et al., 2021; Segawa et al.,
67 2017; Uetake et al., 2019). On glacier ice surface, algae from the order Zygnematales, including
68 *Ancylonema nordenskiöldii*, *Ancylonema alaskanum*, and *Cylindrocystis brébissonii*, are the
69 predominant taxa (Remias et al., 2012; Ling and Seppelt, 1990; Uetake et al., 2010; Takeuchi et al.,
70 2013). In contrast, snow surfaces are mainly inhabited by green and red algae belonging to the order
71 Chlamydomonadales, such as *Chlamydomonas* sp., *Chloromonas* sp., and *Sanguina nivaloides* (Davey
72 et al., 2019; Segawa et al., 2018). Given their patchy and heterogeneity, it is essential to investigate the
73 altitudinal and seasonal variability of their distribution and abundance to improve our understanding of
74 their contributions to carbon cycling and glacier mass balance.

75 Urumqi Glacier No.1, located in the eastern Tien Shan Mountains, is frequently subject to dust
76 storms that derive from surrounding deserts, resulting in substantial deposition of mineral particles on
77 its ablation surface (Nagatsuka et al., 2014). These dust inputs foster the rapid formation and
78 enlargement of cryoconite granules. A previous investigation has reported high areal coverage and
79 biomass of cryoconite on ablation zone of this glacier, which is far exceeding observed on many Arctic
80 glaciers (Takeuchi and Li, 2008). Within these granules, three morphologically distinct filamentous
81 cyanobacterial taxa have been identified (Segawa et al., 2017); each potentially plays a different role in
82 the initiation and structural development of granules (Chen et al., 2025). Moreover, micro-scale
83 biogeochemical analyses have revealed active nitrogen cycling processes within cryoconite (Segawa et
84 al. 2014, 2020; Murakami et al., 2022), suggesting the presence of nutrient hotspots that sustain
85 microbial life on the oligotrophic supraglacial environment. However, previous studies have focused
86 almost exclusively on the single time-point observations of cryoconite and ablation zone, with limited
87 insight into the temporal dynamics of microbial communities across snow and ice surfaces during the
88 melt season. Furthermore, although hydrological and meteorological observations on this glacier have
89 been conducted since the 1960s (Dong et al., 2012), continuous monitoring of microbial community



90 dynamics has never been carried out, and the influence of biological processes on surface albedo has
91 not been adequately considered. Therefore, conducting continuous observations during the biologically
92 active melt season is essential for improving the accuracy of mass balance models and enhancing our
93 understanding of bio-albedo feedbacks in glacier retreat.

94 This study has three main objectives: (1) to investigate the spatial and temporal distribution patterns
95 of algal and cyanobacterial communities on glacial snow and ice surfaces of Urumqi Glacier No.1; (2)
96 to identify key environmental drivers influencing variations in community structure; and (3) to evaluate
97 the ecological role of phototrophic taxa (algae and cyanobacteria) and their potential impact on glacier
98 surface albedo.

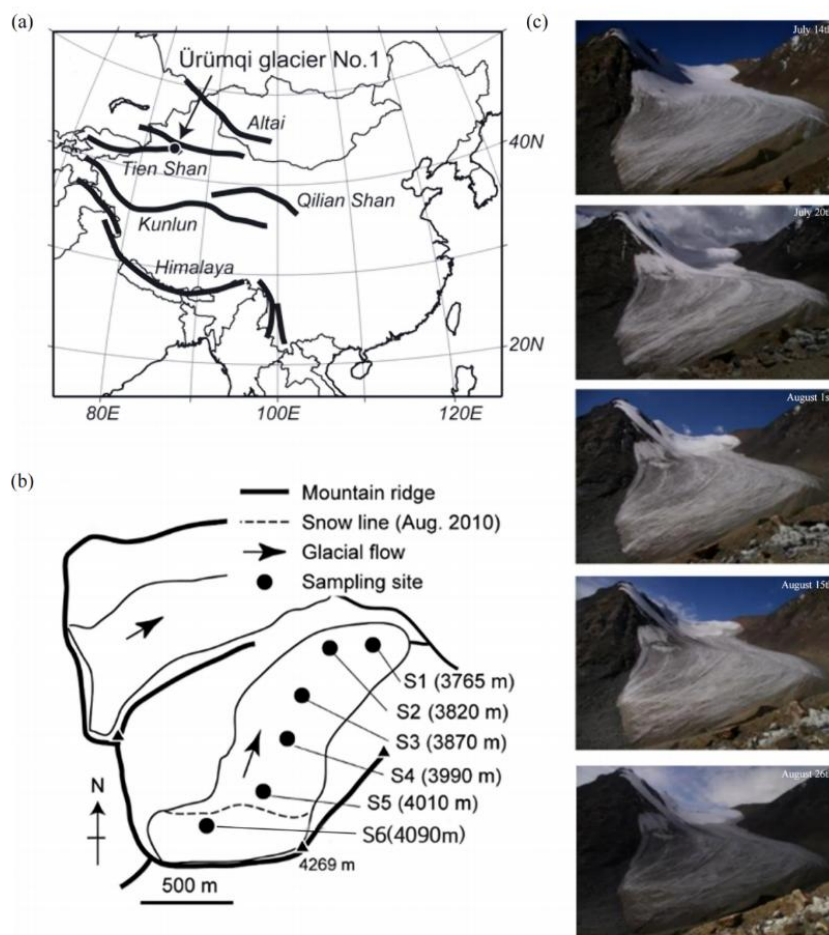
99 **2 Study sites and methods**

100 **2.1 Study sites**

101 Urumqi Glacier No.1, located at 43°06'N and 86°49'E, lies within the Tien Shan Mountains of the
102 Xinjiang Uyghur Autonomous Region in western China (Fig. 1a). This northeast-facing glacier spans
103 elevations from 3,752 to 4,445 m above sea level (a.s.l.). This glacier lost approximately 20% of its
104 volume between 1962 and 2003, and it split into eastern and western branches in 1993 as a result of its
105 continued retreat (Ye et al., 2005). The total catchment area is approximately 1.618 km² (Yue et al.,
106 2022). Mass accumulation primarily occurs during the summer months, corresponding with peak
107 precipitation rates. Hourly meteorological data, including air temperature, downwards solar radiation,
108 precipitation, and snowmelt (in water equivalent), were obtained from ERA5-Land (0.1° × 0.1°
109 resolution, 2 m above surface,
110 <https://cds.climate.copernicus.eu/datasets/reanalysis-era5-land?tab=download>) for July 1 – August 31,
111 2013, and converted to daily means by averaging hourly values (Fig. 2). The mean annual equilibrium
112 line altitude (ELA) in 2013 was 4240 m a.s.l. (https://wgms.ch/products_ref_glaciers/urumqi/). This
113 region is frequently influenced by dust storm activity due to the surrounding major deserts, with dust
114 primarily originating from the Taklimakan Desert (Takeuchi et al., 2011; Li et al., 2010; Nagatsuka et
115 al., 2014). The glacier's ablation zone is notably characterized by the widespread presence of
116 cryoconite granules, with a mean dry weight of 335 g m⁻² and an organic matter content of 9.4 ± 1.6%
117 (Takeuchi and Li, 2008). Cryoconite holes are generally absent from the glacier surface (Takeuchi and

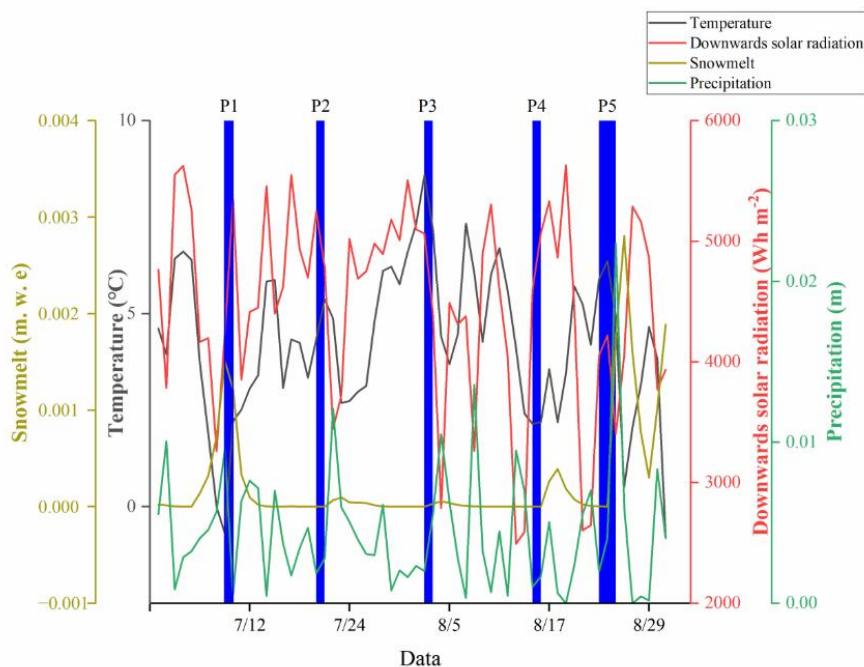


118 Li, 2008).



119

120 **Figure 1: Location maps and photographs of Urumqi Glacier No.1.** (a) Location of Urumqi Glacier No.1 in
121 the Tien Shan Mountains. (b) Map of sampling sites (S1–S6) in this study. (c) Photographs of Urumqi
122 Glacier No.1 across five sampling periods in 2013.



123

124 **Figure 2: Meteorological datasets of Urumqi Glacier No.1 during July and August in 2013. P1-P5 denote**
 125 **sampling period.**

126 **2.2 Methods**

127 **2.2.1 Sampling collection**

128 Field investigations were conducted five times in 2013, specifically on July 8–11 (P1), July 20–21 (P2),
 129 August 2–3 (P3), August 15–16 (P4), and August 24–26 (P5), across six sites on different altitudes
 130 (S1-S6, Fig. 1b). During P1, S1–S4 were characterized by exposed ice surfaces, while S5 and S6
 131 remained snow-covered (Fig. 1c). In the subsequent four sampling periods, ice surfaces extended
 132 upslope, resulting in S1 to S5 being classified as ice surfaces, with only S6 retaining a snow cover (Fig.
 133 1c). Surface ice and snow samples, approximately 1–2 cm in thickness, were collected along the
 134 eastern branch of Urumqi Glacier No.1 using a pre-cleaned stainless-steel scoop. For subsequent
 135 analysis, three to five samples were collected from randomly selected surface areas at each site. To
 136 preserve biological activity, samples were melted and fixed with a 3% formalin solution in sterile 30
 137 mL polyethylene bottles (IBOY, AS ONE, Japan). Additionally, one sample per site was collected and
 138 kept frozen without fixative for taxonomic identification of algal and cyanobacterial species. All



139 samples were subsequently delivered to a laboratory at Chiba University for further analysis.

140 **2.2.2 Quantification of algal and cyanobacterial biomass**

141 Biomass of algae and cyanobacteria at each sampling site was quantified via direct cell counting using
142 an optical microscope. To loosen sedimentary particles, each sample was ultrasonicated for 10 minutes.
143 A volume of 2–100 mL of meltwater was filtered through a polytetrafluoroethylene (PTFE) membrane
144 filter (pore size 0.45 μm ; JHWP01300, Merck Millipore, Germany), and cells retained on the filter
145 were enumerated using an optical microscope (BX51, Olympus, Japan) by counting 1–3 randomly
146 selected transects per filter. Only cells showing chlorophyll autofluorescence were considered as active
147 cells and included in the counts. Each sample was counted in 3–5 times to ensure reproducibility. Cell
148 concentrations (cells mL^{-1}) were calculated based on the average cell counts and the volume of water
149 filtered. Total biomass ($\mu\text{L m}^{-2}$) of algae and cyanobacteria was then estimated by bio-volume (cell
150 volume) per unit surface area. The biovolume was calculated from the volumes of geometric analogs of
151 cell morphology: cyanobacterial cells were modeled as cylinders, and algal cells were represented as
152 ellipsoids or spheres, depending on their morphology. Mean cell volume for each taxon was determined
153 by measuring the dimensions of 50 individual cells per taxon. The morphological taxa composition
154 (proportion) at each site was expressed as the relative abundance of each taxon to the total bio-volume.
155 Mean values and standard deviations were calculated based on replicate samples collected from
156 different surface areas at each site.

157 **2.2.3 Major chemical solutes measurement**

158 Major soluble ions in snow samples, including anions of NO_3^- , Cl^- , and SO_4^{2-} and cations of NH_4^+ , K^+ ,
159 Na^+ , Mg^{2+} , and Ca^{2+} , were analyzed using an ion chromatography system (ICS-1100, Thermo Fisher
160 Scientific, USA). Prior to analysis, melted samples were filtered through ion-free chromatographic
161 discs (Chromate disk, pore size: 0.45 μm , GL Science, Japan) to eliminate particulate matter.

162 For anion analysis, a Dionex IonPac AS12A analytical column paired with an AG12A guard column
163 was employed. The eluent consisted of a mixture of 2.7 mM Na_2CO_3 and 0.3 mM NaHCO_3 , delivered at
164 a flow rate of 1.5 mL min^{-1} . For cation analysis, a Dionex IonPac CS12A column was used with 20 mM
165 methanesulfonic acid as the eluent, operating at a flow rate of 1.0 mL min^{-1} .



166 **2.2.4 Statistical data analysis**

167 Dissimilarities in community composition of algae and cyanobacteria, as well as in ion composition
168 across sampling period and surface status, were assessed using permutational multivariate analysis of
169 variance (PERMANOVA) based on Bray–Curtis distance matrices, implemented with the *adonis*
170 function in the R package “*vegan*” (Oksanen et al., 2010). Spearman's rank correlation analysis was
171 conducted in OriginPro to examine relationships between algal/cyanobacterial biomass and chemical
172 variables. Differences in total biomass and ion concentrations among sampling periods and surface
173 conditions were evaluated using one-way analysis of variance (ANOVA) in OriginPro. Statistical
174 significance was determined at $p < 0.05$.

175 **3 Results**

176 **3.1 Observed algae and cyanobacteria on the glacier surface**

177 Two taxa of algae and six taxa of cyanobacteria were identified on the glacier surface through
178 microscopic observation (Fig. 3). The morphological characteristic of each taxon was described as
179 follows, in conjunction with findings from previous DNA-based studies (Segawa et al., 2017; 2023).
180 Molecular analyses previously detected a total of 20 cyanobacterial operational taxonomic units (OTUs)
181 on the glacier surface.

182 **Algae**

183 **(1) *Chloromonadinia* species**

184 Cells were spherical in shape and lacked visible pyrenoids in the chloroplasts. Intracellular pigments
185 appeared green and red, and all observed cells were in the zygote stage. Mean cell diameter was $16.0 \pm$
186 $1.8 \mu\text{m}$. Based on previously reported DNA metabarcoding data from this glacier, which showed that
187 members of *Chloromonadinia* were highly abundant in snow samples (Segawa et al., 2023), these
188 morphotypes were therefore assigned to *Chloromonadinia* species.

189 **(2) *Cylindrocystis brébissonii***

190 Cells were cylindrical with rounded apices, containing two chloroplasts each with a central pyrenoid.
191 However, only one chloroplast was observed in short, divided cells. Cells measured $28.3 \pm 6.0 \mu\text{m}$ in
192 length and $17.6 \pm 1.9 \mu\text{m}$ in width.

193 **Cyanobacteria**



194 **(1) Oscillatoriaceae (Osc.) cyanobacteria 1**

195 Trichomes lacked a sheath, and clear constrictions were visible between adjacent cells. Mean cell
196 diameter was $1.6 \pm 0.2 \mu\text{m}$. This morphotype corresponded to OTU5 (*Pseudanabaena*) (Segawa et al.,
197 2017).

198 **(2) Oscillatoriaceae cyanobacteria 2**

199 Trichome were enclosed within a colorless mucilaginous sheath. Green intracellular granules were
200 observed within the cells. Mean cell diameter was $3.1 \pm 0.5 \mu\text{m}$. This morphotype corresponded to
201 OTU4 (*Microcoleus*) species (Segawa et al., 2017).

202 **(3) Oscillatoriaceae cyanobacterium 3**

203 Trichome were surrounded by a colorless mucilaginous sheath, without conspicuous internal structures.
204 Mean cell diameter was $1.5 \pm 0.2 \mu\text{m}$, This morphotype identified as OTUs 0 (unclassified), 8
205 (*Oscillatoriales*), and 9 (*Geitlerinema*) (Segawa et al., 2017).

206 **(4) Chroococcaceae (Chr.) cyanobacterium 1**

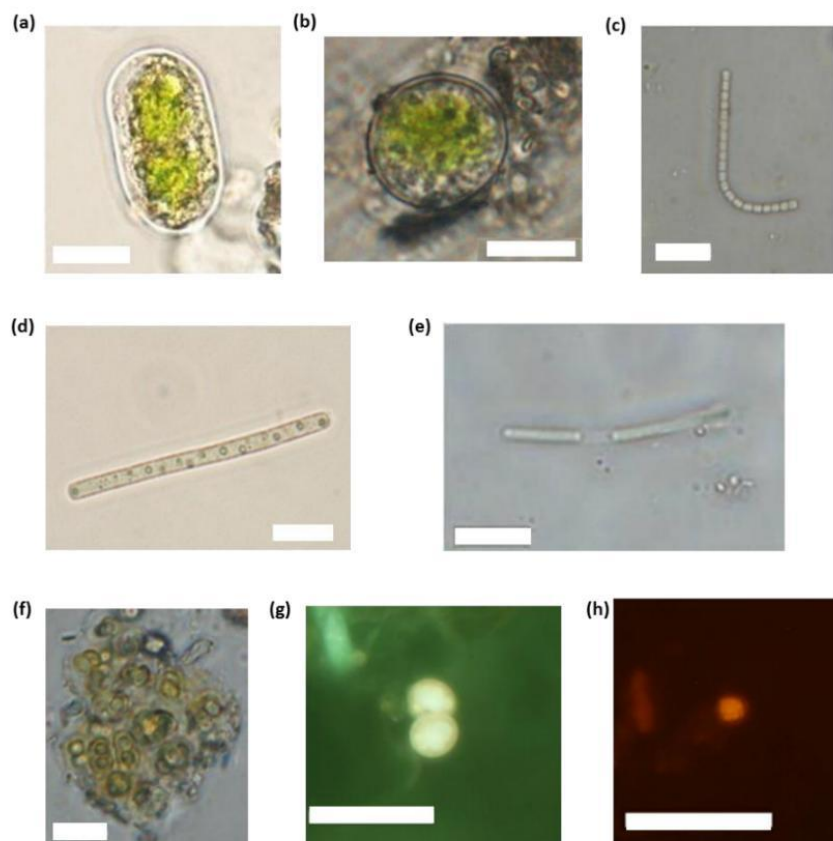
207 Spherical cells were surrounded by with brown or yellow mucilaginous sheaths and occurred as
208 solitary or paired cells forming small colonies. Mean cell diameter was $3.8 \pm 0.6 \mu\text{m}$.

209 **(5) Chroococcaceae cyanobacterium 2**

210 Spherical paired cells without apparent colonies. Mean cell diameter was $3.9 \pm 0.6 \mu\text{m}$.

211 **(6) Chroococcaceae cyanobacterium 3**

212 Spherical cells with a mean diameter of $2.7 \pm 1.1 \mu\text{m}$.



(g) and (h) were observed with a fluorescent microscope.

213

214 **Figure 3: Photographs of algae and cyanobacteria observed on surface of Urumqi Glacier No.1.** (a)
215 *Cylindrocystis brébissonii*; (b) *Chloromonadinia* species; (c) Oscillatoriaceae cyanobacterium 1; (d)
216 Oscillatoriaceae cyanobacterium 2; (e) Oscillatoriaceae cyanobacterium 3; (f) Chroococcaceae
217 cyanobacterium 1; (g) Chroococcaceae cyanobacterium 2; (h) Chroococcaceae cyanobacterium 3. Scale bar
218 = 10 μm

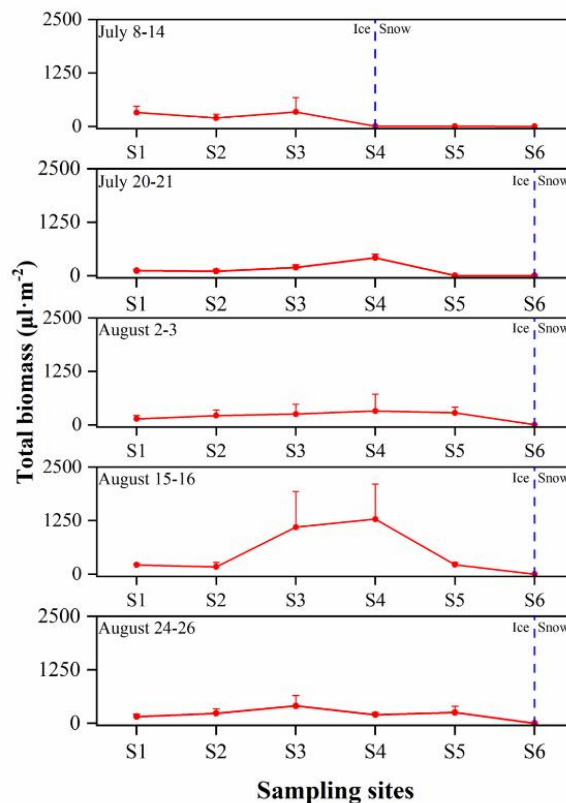
219 3.2 Seasonal and spatial variations in the total biomass of algae and cyanobacteria

220 The total bio-volume biomass of algae and cyanobacteria on the glacier surface remained relatively
221 stable through the melt season (One-way ANOVA, $F = 0.007$, $p = 0.9 > 0.05$, Fig. 4). However, a
222 marked increase in total biomass was observed when the snow surface transitioned to bare ice at the
223 midstream sites (S4 and S5). At S4, biomass increased markedly from $4.7 \times 10^{-3} \text{ mL m}^{-2}$ in P1 to
224 0.42 mL m^{-2} in P2. At S5, although the biomass in P1 ($3.7 \times 10^{-3} \text{ mL m}^{-2}$) was not significantly
225 different from that in P2 ($1.2 \times 10^{-3} \text{ mL m}^{-2}$), a significant increase was observed in P3, with biomass



226 reaching 0.28 mL m^{-2} . Furthermore, the total biomass on the ice surface was significantly higher than

227 that on the snow surface (One-way ANOVA, $F = 23.2$, $p < 0.01$).



228

229 **Figure 4: Seasonal and spatial variations in the total bio-volume biomass of algae and cyanobacteria on**
 230 **Urumqi Glacier No.1 from July to August 2013. The dashed line represents the boundary between the snow**
 231 **and ice surface.**

232 **3.3 Spatiotemporal changes of algal and cyanobacterial community composition on glacier**
 233 **surfaces**

234 The relative dominance of algae and cyanobacteria varied with both sampling period and surface status
 235 (Fig. 5). PERMANOVA analysis indicated no significant differences ($p > 0.05$) in community
 236 composition across the different sampling periods but significant differences were found between snow
 237 and ice surfaces (PERMANOVA, $p < 0.01$). Specifically, algal taxa, primarily *Chloromonadinia*
 238 species, strongly dominated snow-covered surfaces, while cyanobacteria were consistently the
 239 dominant on bare ice surfaces throughout the study.

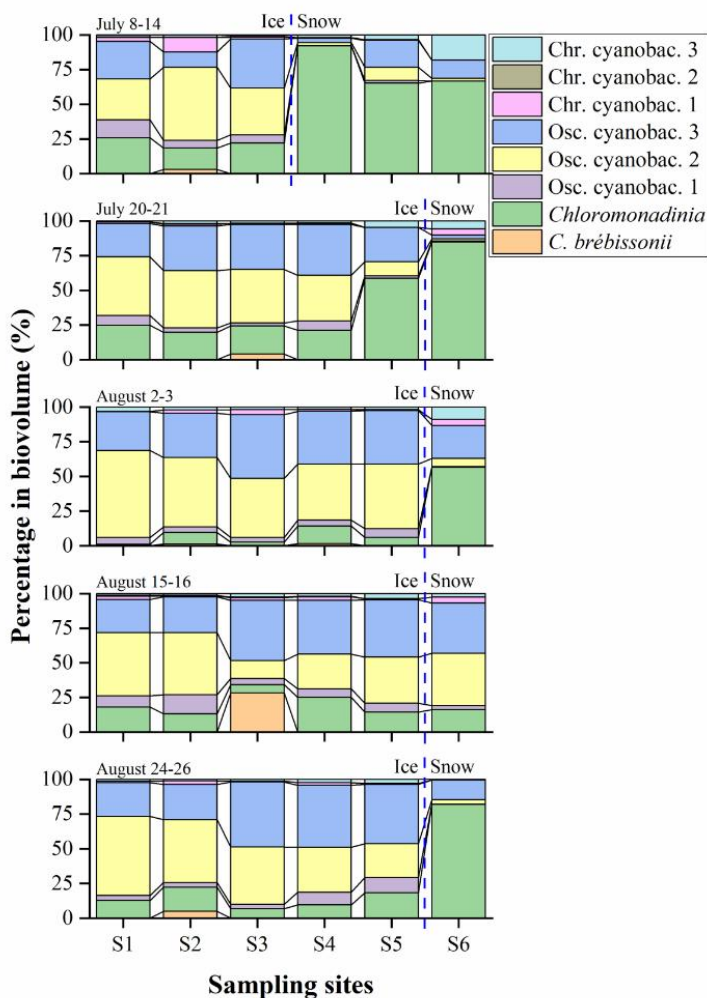


240 In P1, filamentous cyanobacteria were dominant on ice surfaces of the downstream sites (S1 to S3),
241 accounting for 61–75% of the total biomass, whereas the snow-covered upstream sites (S4 to S6) were
242 prevailed by *Chloromonadina* species, contributing 65–92% of the total biomass. By P2, the upstream
243 expansion of bare ice was accompanied by a corresponding upstream shift in cyanobacterial dominance,
244 leaving *Chloromonadina* species predominant only at S5 and S6. From P3 onward, filamentous
245 cyanobacteria consistently dominated from S1 to S5, while *Chloromonadina* species remained
246 dominant solely at the uppermost site, S6. For instance, in P5, filamentous cyanobacteria comprised
247 77–93% of the total biomass at S1 to S5, while *Chloromonadina* species accounted for 82% at S6. An
248 exception occurred in P4, during which filamentous cyanobacteria were dominant across all sites,
249 comprising 61–84% of the total biomass.

250 *Cylindrocystis brébissonii* was exclusively detected on ice surfaces and was sporadically observed in
251 one or two samples per sampling period. In P1, it was present at S2, accounting for 6% of the total
252 biomass. In P2, the alga was observed at S3, contributing 8% of the total biomass. In P3, the taxon was
253 detected at S2 and S4, accounting for 3% and 5% of the biomass, respectively. Its highest relative
254 abundance was observed in P4 at S3, where it constituted 28% of the total biomass. In P5, it was
255 present again at S2, comprising 5% of the total biomass.

256 *Osc.* cyanobacterium 1 showed a clear preference for ice surfaces, with biomass generally rising
257 from P1 to P4, particularly at mid- to up-glacier ice sites. Its presence on snow surfaces was negligible
258 across all periods, rarely exceeding $0.1 \mu\text{L m}^{-2}$.

259 *Osc.* cyanobacteria 2 and 3 were the dominant cyanobacterial taxa on ice surfaces throughout the
260 study period, constituting 65%–95% of the total cyanobacterial biomass across all ice sites and
261 sampling periods. Their biomass increased progressively from P1 to P4, with the highest values
262 recorded at sites S3 and S4 during P4, where *Osc.* cyanobacterium 2 exceeded $300 \mu\text{L m}^{-2}$ and *Osc.*
263 cyanobacterium 3 surpassed $470 \mu\text{L m}^{-2}$. From P4 onward, a distinct spatial pattern emerged: *Osc.*
264 cyanobacterium 2 dominated the downstream sites (S1–S2), whereas *Osc.* cyanobacterium 3 became
265 dominant at the upstream sites (S3–S5). In contrast, both taxa were nearly absent on snow-covered
266 surfaces, with biomass consistently below $1 \mu\text{L m}^{-2}$.



267

268 **Figure 5: Seasonal and spatial variations in the morphological community structure of algae and**
 269 **cyanobacteria at study sites S1–S6 on Urumqi Glacier No.1 from July to August 2013. The dashed line**
 270 **represents the boundary between the snow and ice surface.**

271 Among the unicellular cyanobacteria, Chr. cyanobacterium 1 showed a noticeable biomass increase
 272 by P4 on ice, reaching up to $\sim 30 \mu\text{L m}^{-2}$ at sites S3 and S4. Chr. cyanobacteria 2 and 3 maintained
 273 relatively low abundance levels throughout all sampling sites and periods, with slight elevations
 274 observed on ice during P4. All three Chroococcaceae taxa were almost absent on snow surfaces
 275 (biomass $< 0.13 \mu\text{L m}^{-2}$).

276

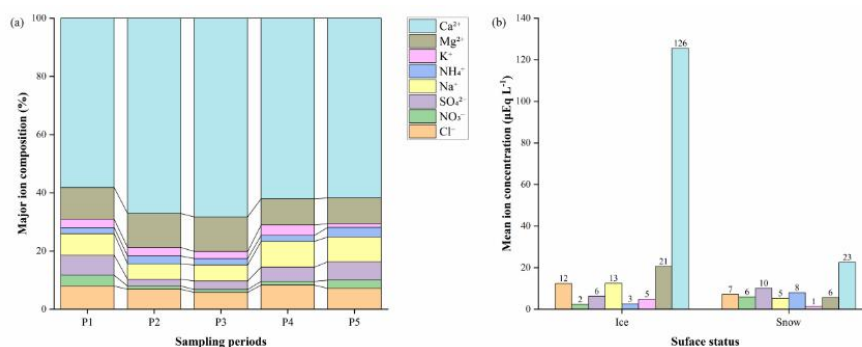


277 **3.4 Variations in chemical conditions across the sampling period and surface status**

278 The concentrations of major ions showed notable temporal variation throughout the five sampling
 279 periods. Ca²⁺ consistently dominated the ionic composition, accounting for more than 58.3% of the
 280 total ion content, while the relative proportions of other ions fluctuated over time (Fig. 6a).

281 SO₄²⁻, NO₃⁻, K⁺ and Mg²⁺ concentrations temporally varied significantly among sampling periods
 282 (one-way ANOVA, p < 0.01). SO₄²⁻ and NO₃⁻ both peaked in P1 (= 12.9 and = 6.8 μEq L⁻¹,
 283 respectively), declined sharply in P2, and showed secondary increases in P5. In contrast, K⁺ remained
 284 stable in early periods (~5 μEq L⁻¹) before declining to its lowest level in P5 (= 1.7 μEq L⁻¹). Mg²⁺
 285 exhibited elevated concentrations in P1 and P3 (= 20.3 and = 25.9 μEq L⁻¹), dropped markedly in P4,
 286 and partially rebounded in P5.

287 Significant differences in ion concentrations were also observed between surface status (ice vs. snow)
 288 (one-way ANOVA, p < 0.01, Fig. 6b). Ice surfaces consistently hold higher mean concentrations of
 289 crustally derived ions, including Ca²⁺ (125.5 vs. 22.6 μEq L⁻¹), Mg²⁺ (20.6 vs. 5.9 μEq L⁻¹), Na⁺ (12.5
 290 vs. 5.3 μEq L⁻¹) and K⁺ (4.9 vs. 1.3 μEq L⁻¹). In contrast, snow surfaces showed higher concentrations
 291 of NO₃⁻ (2.3 vs. 6.0 μEq L⁻¹), SO₄²⁻ (6.3 vs. 10.1 μEq L⁻¹), and NH₄⁺ (2.6 vs. 8.0 μEq L⁻¹).



292
 293 **Figure 6: (a) Major ion composition in surface snow and ice at five sampling period (P1–P5). (b)**
 294 **Comparison of mean ion concentrations between snow and ice surfaces.**

295 **4 Discussion**

296 **4.1 Algal community dynamics in response to glacier surface transition**

297 The algal biomass on Urumqi Glacier No.1 remained consistently low with minimal temporal variation,
 298 suggesting that algal proliferation is highly constrained in this environment. *Chloromonadina* species



299 was found on both snow and ice but showed a clear preference for snow, aligning with its classification
300 as a snow-environment specialist (Takeuchi, 2001), similar to observations in the Himalayas
301 (Yoshimura et al., 1997) and Altai Mountains (Takeuchi et al., 2006). Conversely, the green alga *C.*
302 *brébissonii* was restricted to ice surfaces. Despite its presence, its sporadic and low abundance suggest
303 it functions as an ice-specialist that fails to establish stable, large-scale populations on this glacier,
304 contrasting with earlier classifications that often regard certain *Cylindrocystis* strains as opportunists
305 with broader habitat ranges (Kol, 1942; Remias et al., 2012).

306 On this glacier, the role of algae in surface darkening is habitat-dependent. On snow, despite low
307 biomass, *Chloromonadina* species is likely the primary biological agent for albedo reduction due to
308 the absence of cryoconite. However, on bare ice, the albedo-reducing effect of algae is negligible
309 compared to the pronounced darkening mediated by cyanobacteria and mineral particles. This is
310 consistent with studies suggesting that while snow algae can significantly lower albedo in the early
311 melt season, their impact is often overshadowed by other light-absorbing particles once the ice is
312 exposed (Lutz et al., 2016; Di Mauro et al., 2020).

313 **4.2 Cyanobacterial dominance and its role in surface darkening**

314 In contrast to the ephemeral nature of snow algae, the cyanobacterial community on Urumqi Glacier
315 No. 1 exhibited remarkable temporal stability in total biomass, albeit with significant spatial and
316 taxonomic shifts. While unicellular Chroococcaceae showed low and variable biomass, filamentous
317 cyanobacteria (Oscillatoriaceae) maintained sustained dominance on ice surfaces throughout the melt
318 season. This persistent presence of filamentous taxa underscores their critical role in surface darkening
319 through two synergistic mechanisms: direct pigmentation and the structural aggregation of mineral
320 particles into dark cryoconite granules.

321 The spatial distribution of these dominant filamentous cyanobacteria revealed a distinct altitudinal
322 zonation from P4 onwards, despite the relatively uniform geochemical characteristics across the glacier.
323 Osc. cyanobacterium 2 dominated the downstream sites (S1–S2), while Osc. cyanobacterium 3
324 prevailed at the mid-to-up-glacier sites (S3–S5). Given the lack of significant chemical gradients, this
325 niche partitioning is likely driven by physical factors associated with altitude, specifically the duration
326 of bare-ice exposure and the frequency of summer snowfall. The downstream sites (S1–S2) experience
327 the earliest snow disappearance and the longest continuous melt season, allowing for the development



328 of "mature" cryoconite communities. *Osc. cyanobacterium 2* appears to be a late-successional specialist,
329 capable of maintaining high biomass under conditions of prolonged meltwater flow and cumulative
330 dust aggregation. Its dominance at lower altitudes suggests a high tolerance to the physical stability of
331 older cryoconite granules in the stable, long-term habitats of the lower ablation zone. In contrast, the
332 mid-to-up-glacier sites (S3–S5) encounter a much shorter exposure window and are frequently
333 subjected to transient snow cover, which resets the surface temperature and temporarily halts microbial
334 activity. The dominance of *Osc. cyanobacterium 3* in these areas—marked by an explosive biomass
335 increase exceeding $470 \mu\text{L m}^{-2}$ during P4—suggests it is a "pioneer-like" rapid colonizer. This taxon
336 likely possesses physiological traits suited for rapid growth immediately following ice exposure or a
337 higher resilience to the frequent freeze-thaw cycles and intermittent snow cover characteristic of higher
338 altitudes.

339 This altitudinal segregation implies that the cyanobacterial community is not a monolithic
340 assemblage but a strategically partitioned system. The presence of multiple dominant taxa with
341 different spatio-temporal peaks ensures that the glacier surface maintains high biological biomass
342 across a wide range of environmental conditions—from stable lower reaches to dynamic, intermittently
343 snow-covered upper reaches. Such functional diversity within the Oscillatoriaceae ensures that the
344 biological darkening effect is not localized or transient but remains stable and continuous across the
345 entire ablation zone.

346 Unlike the ephemeral algal blooms observed on Arctic glaciers (Takeuchi, 2013), where darkening is
347 highly sensitive to the seasonal timing of snowmelt, the biological impact on Urumqi Glacier No. 1 is
348 stabilized by the formation and persistence of cryoconite granules. Filamentous cyanobacteria produce
349 extracellular polymeric substances (EPS) that trap mineral dust, creating the dark, spherical aggregates
350 characteristic of this region (Musilova et al., 2016; Segawa et al., 2017). A critical distinction is that
351 these granules are not merely seasonal features; they can persist and grow over multiple melting
352 seasons, effectively serving as long-term reservoirs for both mineral and organic matter. This
353 multi-year development facilitates the accumulation of refractory organic compounds, such as humic
354 substances, which significantly enhance the light-absorbing capacity of the granules (Takeuchi, 2002).

355 The structural stability provided by the cyanobacterial matrix ensures that these dark, humic-rich
356 aggregates remain on the ice surface even during intermittent snowfall or minor scouring events. Given
357 that such consolidated cryoconite granules exert a stronger and more localized albedo-reducing effect



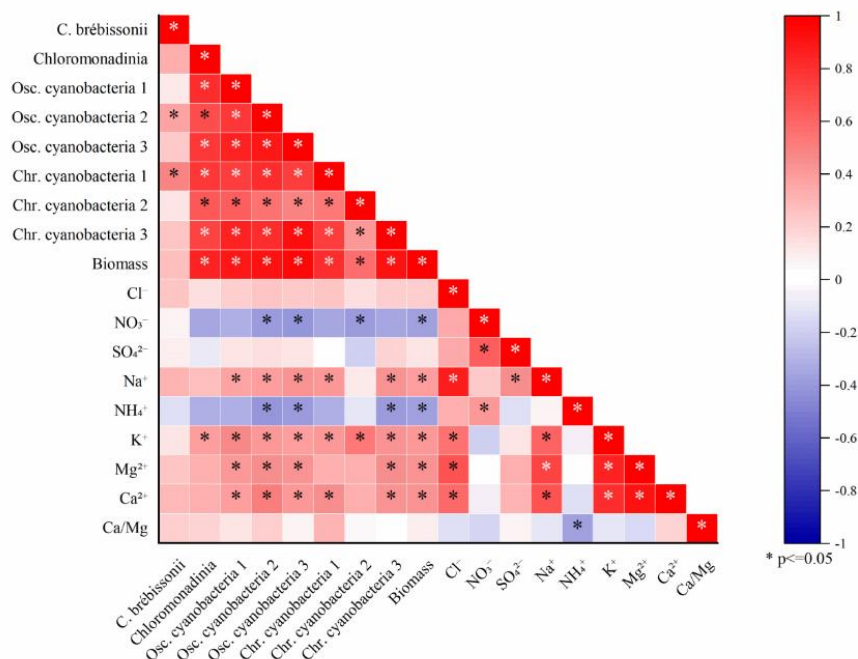
358 than the transient, distributed blooms of snow or ice algae (Cook et al., 2016; Hotaling et al., 2021), the
359 "cyanobacteria-mineral synergy" driven by these specialized filamentous taxa represents the primary
360 biological mechanism for persistent and cumulative surface darkening in Central Asian glaciers.

361 **4.3 Environmental drivers: Nitrogen limitation and mineral-derived ions**

362 The distinct community compositions on snow and ice surfaces suggest different environmental
363 controls. We found significant negative correlations between inorganic nitrogen concentrations (NO_3^-
364 and NH_4^+) and the relative abundance of dominant filamentous cyanobacteria (Oscillatoriaceae) ($p <$
365 0.05 ; Fig. 7). This suggests that nitrogen-poor ice surfaces favor these cyanobacteria, which are known
366 to harbor metabolic pathways for efficient nitrogen utilization and recycling within the stable
367 micro-habitats of cryoconite granules (Segawa et al., 2014; 2020; Murakami et al., 2022).

368 Furthermore, Oscillatoriaceae biomass positively correlated with mineral-derived ions (Ca^{2+} , Mg^{2+} ,
369 and K^+ , $p < 0.05$, Fig. 7), which serve as proxies for mineral dust abundance (Li et al., 2010; Nagatsuka
370 et al., 2014). The concentrations of these ions on Urumqi Glacier No.1 are substantially higher than
371 those reported for Arctic glaciers, such as those in Svalbard, where mineral-derived ion concentrations
372 are significantly lower due to limited dust input (Takeuchi et al., 2019). While the low-mineral
373 environment of Svalbard glaciers typically favors the dominance of glacier algae on the ice surface, the
374 high mineral availability on Urumqi Glacier No.1 provides a more suitable substrate and nutrient base
375 for the proliferation of filamentous cyanobacteria and the subsequent development of cryoconite
376 granules. This stark contrast in geochemical conditions explains why the primary biological drivers of
377 albedo reduction differ so fundamentally between Central Asian and Arctic glacial systems.

378 This relationship highlights the critical importance of mineral availability for cyanobacterial
379 colonization and granule formation. Our results mirror observations from the Greenland Ice Sheet,
380 where phosphorus and mineral availability are key drivers of cyanobacterial growth (Uetake et al.,
381 2019; McCutcheon et al., 2021), but this effect is likely amplified on Urumqi Glacier No.1 due to the
382 extreme dust deposition characteristic of Central Asian mountains. In contrast, algal taxa showed no
383 such correlations, suggesting their distribution may be driven by stochastic colonization or micro-scale
384 physical factors like meltwater flow rather than macro-scale chemical parameters (Stibal et al., 2012a).



385

386 **Figure 7: Correlation between major ion concentration and bio-volume of each algal and cyanobacterial**
 387 **taxa.**

388 **4.4 Ecological Implications and comparison with Arctic glaciers**

389 One of the most significant ecological findings of this study is the complete absence of glacier algae,
 390 such as *Ancylonema* spp., which are the primary drivers of ice darkening on Arctic glaciers (e.g.,
 391 Alaska, Svalbard) (Takeuchi 2013; Takeuchi et al., 2019). In polar regions, these Zygnematalean algae
 392 bloom on the ice surface, producing dark purple pigments that significantly reduce albedo (Williamson
 393 et al., 2018; Remias et al., 2012). However, on Urumqi Glacier No.1, this niche is entirely occupied by
 394 a stable, cyanobacteria-dominated community.

395 The absence of *Ancylonema* and the corresponding dominance of filamentous cyanobacteria
 396 (*Oscillatoriaceae*) are likely attributable to the unique geochemical and physical environment of
 397 Central Asia. Takeuchi et al. (2019) demonstrated that Arctic glaciers in Svalbard are characterized by
 398 extremely low mineral ion concentrations, a condition that appears to favor the proliferation of
 399 free-living glacier algae. In contrast, the high dust flux on Urumqi Glacier No.1 provides an abundance
 400 of mineral cations, resulting in substantially elevated ionic concentrations. For example, mean Mg^{2+}



401 and Ca^{2+} concentrations on Urumqi Glacier No. 1 are approximately 13 and 59 times higher,
402 respectively, than those reported for Svalbard (Mg^{2+} : 20.6 vs. 1.6 $\mu\text{Eq L}^{-1}$; Ca^{2+} : 125.5 vs. 2.1 $\mu\text{Eq L}^{-1}$).
403 These elevated mineral inputs not only raises the ionic strength but may also maintain a higher pH on
404 the ice surface. Central Asian glaciers are characterized by a high influx of mineral dust containing
405 abundant carbonate minerals, particularly calcite (CaCO_3), from the surrounding arid regions (Li et al.,
406 2010; Nagatsuka et al., 2014). The dissolution of these carbonate-rich particles consumes protons and
407 releases bicarbonate (HCO_3^-), acting as a powerful geochemical buffer that maintains the meltwater pH
408 in a neutral to alkaline range (typically pH 7.5–8.5), as documented in hydrochemical studies of
409 Urumqi Glacier No. 1 (Li et al., 2007; Wu et al., 2012). Such alkaline and mineral-rich conditions may
410 be physiologically inhibitory to *Ancylonema*, which typically thrives in the more acidic,
411 ultra-oligotrophic environments characteristic of polar ice (Remias et al., 2012; McCutcheon et al.,
412 2021).

413 Furthermore, the physical presence of massive mineral dust promotes the formation of cryoconite
414 granules. As revealed by Segawa and Takeuchi (2010) on Qiyi Glacier and further elucidated by Chen
415 et al. (2025) on Urumqi Glacier No.1, filamentous cyanobacteria act as "ecosystem engineers,"
416 trapping mineral particles to form stable, spherical aggregates. This process may physically exclude
417 glacier algae by reducing the availability of "clean" ice surfaces required for their colonization.

418 These results suggest that the biological darkening of Central Asian glaciers follows a fundamentally
419 different mechanism—a "cyanobacteria-mineral synergy"—compared to the "algal bloom" model of
420 the Arctic. While Arctic darkening is often ephemeral and sensitive to seasonal snowmelt timing, the
421 darkening on Urumqi Glacier No.1 is more persistent due to the structural stability of cyanobacterial
422 cryoconite. Therefore, applying Arctic-based bio-albedo models to Central Asian glaciers may lead to
423 significant errors, highlighting the need for region-specific models that account for high mineral
424 loading and its role in shaping microbial community structures.

425 **5 Conclusion**

426 This study characterized the spatiotemporal dynamics of phototrophic communities on Urumqi Glacier
427 No. 1, revealing an ecological structure fundamentally distinct from those of better-studied polar
428 glacial systems. The primary finding of this research is the clear biological succession driven by the
429 seasonal transition of the glacier surface. As the snowpack recedes, the community shifts from the



430 dominance of the snow alga *Chloromonadina* species to a massive proliferation of filamentous
431 cyanobacteria (Oscillatoriaceae) on the exposed bare ice. This transition is marked by a significant
432 increase in total biomass and the establishment of a stable microbial community that persists
433 throughout the ablation period.

434 Crucially, this study highlights the complete absence of glacier algae such as *Ancylonema* spp.,
435 which are the primary drivers of ice darkening on Arctic glaciers. Instead, the biological darkening on
436 Urumqi Glacier No.1 is governed by a specialized "cyanobacteria-mineral synergy." Our results
437 demonstrate that the proliferation of dominant filamentous cyanobacteria is closely linked to high
438 concentrations of mineral-derived ions and low inorganic nitrogen levels. This geochemical
439 environment, shaped by high dust input from surrounding arid regions, appears to provide a specialized
440 niche that favors cyanobacterial colonization and the structural development of cryoconite granules
441 over the growth of eukaryotic glacier algae. Furthermore, we identified an altitudinal niche partitioning
442 within the Oscillatoriaceae, where different taxa (e.g., Osc. cyanobacterium 2 and 3) dominate based on
443 the duration of ice exposure and snowfall frequency. This functional diversity ensures that a high
444 biological biomass is maintained across the entire ablation zone, regardless of altitudinal gradients.

445 The ecological implications of these findings are essential for predicting the future of alpine glaciers
446 in a changing climate. Unlike the ephemeral algal blooms observed in Arctic regions, the darkening on
447 Urumqi Glacier No. 1 is driven by structurally stable cryoconite granules that can persist and grow over
448 multiple melt seasons. This multi-year development facilitates the accumulation of refractory humic
449 substances, creating a more constant, cumulative, and resilient bio-albedo feedback mechanism. Under
450 projected warming scenarios, including extended melt seasons and increased dust deposition, the
451 expansion of these cyanobacterial communities may further accelerate glacier mass loss. Therefore, it
452 is imperative to integrate region-specific microbial dynamics—characterized by the absence of glacier
453 algae and the dominance of mineral-buffered, long-lived cyanobacterial aggregates—into global glacier
454 melt models to improve the accuracy of water resource projections in Central Asia.

455 **Data availability**

456 The datasets generated and analyzed during the current study are available from the corresponding
457 author upon reasonable request.



458 **Author contributions**

459 YC and NT designed the study. YC and NT wrote and revised the manuscript with supports of XH and
460 WZ. ST collected samples and quantified biomass of algae and cyanobacteria. NT measured ion
461 concentration. YC and SL statistically analyzed data and draw Figs. ZL organized the field
462 investigation.

463 **Competing interests**

464 The authors have declared that they have no competing interests in relation to this study.

465 **Disclaimer**

466 Copernicus Publications remains neutral with regard to jurisdictional claims made in the text, published
467 maps, institutional affiliations, or any other geographical representation in this paper. While Copernicus
468 Publications makes every effort to include appropriate place names, the final responsibility lies with the
469 authors. Views expressed in the text are those of the authors and do not necessarily reflect the views of
470 the publisher.

471 **Acknowledgments**

472 We gratefully acknowledge the invaluable support provided by the members of the Northwest Institute
473 of Eco-Environment and Resources, Chinese Academy of Sciences, Lanzhou, China, during the
474 fieldwork. We would also like to show our gratitude to Dr. Zanpin Xin for meteorological data support.

475 **Financial support**

476 This study was financially supported by the JSPS KAKENHI (25K22868, 24H00260, 22H03731, and
477 21H0457) and Young Scientists Fund of the National Natural Science Foundation of China (42306268
478 and 42201056).



479 **References**

- 480 Anesio, A.M. and Laybourn-Parry, J.: Glaciers and ice sheets as a biome, *Trends Ecol. Evol.*, 27,
481 219-225, <https://doi.org/10.1016/j.tree.2011.09.012>, 2012.
- 482 Anesio, A.M., Lutz, S., Christmas, N.A. and Benning, L.G.: The microbiome of glaciers and ice sheets,
483 *npj Biofilms Microbi.*, 3, 10. <https://doi.org/10.1038/s41522-017-0019-0>, 2017.
- 484 Chen, Y., Takeuchi, N., Tanaka, S. and Li, Z.: Aggregation of mineral particles in cryoconite granules
485 by multiple species of cyanobacteria on Urumqi Glacier No. 1, China, *Front. Earth Sci.*, 13, 1596472,
486 <https://doi.org/10.3389/feart.2025.1596472>, 2025.
- 487 Cook, J., Edwards, A., Takeuchi, N. and Irvine-Fynn, T.: Cryoconite: the dark biological secret of the
488 cryosphere, *Prog. Phys. Geog.*, 40, 66-111, <https://doi.org/10.1177/0309133315616574>, 2016.
- 489 Davey, M.P., Norman, L., Sterk, P., Huete-Ortega, M., Bunbury, F., Loh, B.K.W., Stockton, S., Peck,
490 L.S., Convey, P., Newsham, K.K. and Smith, A.G.: Snow algae communities in Antarctica: metabolic
491 and taxonomic composition, *New Phytologist.*, 222, 1242-1255, <https://doi.org/10.1111/nph.15701>,
492 2019.
- 493 Di Mauro, B., Garzonio, R., Baccolo, G., Franzetti, A., Pittino, F., Leoni, B., Remias, D., Colombo, R.
494 and Rossini, M.: Glacier algae foster ice-albedo feedback in the European Alps, *Sci. Rep.*, 10, 4739,
495 <https://doi.org/10.1038/s41598-020-61762-0>, 2020.
- 496 Dong, Z., Qin, D., Ren, J., Li, K. and Li, Z., Variations in the equilibrium line altitude of Urumqi
497 Glacier No. 1, Tianshan Mountains, over the past 50 years, *Chinese Sci. Bull.*, 57, 4776-4783,
498 <https://doi.org/10.1007/s11434-012-5524-1>, 2012.
- 499 Hodson, A., Anesio, A.M., Tranter, M., Fountain, A., Osborn, M., Priscu, J., Laybourn-Parry, J. and
500 Sattler, B.: Glacial ecosystems, *Ecol. Monogr.*, 78, 41-67, <https://doi.org/10.1890/07-0187.1>, 2008.
- 501 Hotaling, S., Lutz, S., Dial, R.J., Anesio, A.M., Benning, L.G., Fountain, A.G., Kelley, J.L.,
502 McCutcheon, J., Skiles, S.M., Takeuchi, N. and Hamilton, T.L.: Biological albedo reduction on ice
503 sheets, glaciers, and snowfields. *Earth-sci. Rev.*, 220, 103728,
504 <https://doi.org/10.1016/j.earscirev.2021.103728>, 2021.
- 505 Hugonnet, R., McNabb, R., Berthier, E., Menounos, B., Nuth, C., Girod, L., Farinotti, D., Huss, M.,
506 Dussailant, I., Brun, F. and Kääb, A.: Accelerated global glacier mass loss in the early twenty-first
507 century, *Nature*, 592, 726-731, <https://doi.org/10.1038/s41586-021-03436-z>, 2021.



- 508 Irvine-Fynn, T.D. and Edwards, A.: A frozen asset: the potential of flow cytometry in constraining the
509 glacial biome, *Cytom. Part A*, 85, 3-7, <https://doi.org/10.1002/cyto.a.22411>, 2014.
- 510 Kol, E. and Taylor, W.R.: The snow and ice algae of Alaska, *Smithsonian Miscellaneous Collections*,
511 101, Smithsonian Institution, 36 pp., 1942.
- 512 Koshima, S., Seko, K., Yoshimura, Y.: Biotic acceleration of glacier melting in Yala glacier, Langtang
513 region, Nepal Himalaya, *IAHS Publ.*, 218, 309-319, 1993.
- 514 Li, X., Li, Z., Ding, Y., Liu, S., Zhao, Z., Luo, L., Pang, H., Li, C., Li, H., You, X. and Wang, F.:
515 Seasonal variations of pH and electrical conductivity in a snow-firn pack on Glacier No. 1, eastern
516 Tianshan, China, *Cold Reg. Sci. Technol.*, 48, 55-63, <https://doi.org/10.1016/j.coldregions.2006.09.006>,
517 2007.
- 518 Li, Z., Li, H., Dong, Z. and Zhang, M.: Chemical characteristics and environmental significance of
519 fresh snow deposition on Urumqi Glacier No. 1 of Tianshan Mountains, China, *Chinese Geogr. Sci.*, 20,
520 389-397, <https://doi.org/10.1007/s11769-010-0412-6>, 2010.
- 521 Ling, H.U. and Seppelt, R.D.: Snow algae of the Windmill Islands, continental Antarctica.
522 *Mesotaenium berggrenii* (Zygnematales, Chlorophyta) the alga of grey snow, *Antarct. Sci.*, 2, 143-148,
523 <https://doi.org/10.1017/s0954102090000189>, 1990.
- 524 Lutz, S., Anesio, A.M., Edwards, A. and Benning, L.G.: Linking microbial diversity and functionality
525 of arctic glacial surface habitats, *Enviro. Microbiol.*, 19, 551-565,
526 <https://doi.org/10.1111/1462-2920.13494>, 2017.
- 527 Lutz, S., Anesio, A.M., Raiswell, R., Edwards, A., Newton, R.J., Gill, F. and Benning, L.G.: The
528 biogeography of red snow microbiomes and their role in melting arctic glaciers, *Nat. Comm.*, 7, 11968,
529 <https://doi.org/10.1038/ncomms11968>, 2016.
- 530 McCutcheon, J., Lutz, S., Williamson, C., Cook, J.M., Tedstone, A.J., Vanderstraeten, A., Wilson, S.,
531 Stockdale, A., Bonneville, S., Anesio, A.M. and Yallop, M.L.: Mineral phosphorus drives glacier algal
532 blooms on the Greenland Ice Sheet, *Nat. Comm.*, 12, 570, <https://doi.org/10.1038/s41467-020-20627-w>,
533 2021.
- 534 Murakami, T., Takeuchi, N., Mori, H., Hirose, Y., Edwards, A., Irvine-Fynn, T., Li, Z., Ishii, S. and
535 Segawa, T.: Metagenomics reveals global-scale contrasts in nitrogen cycling and cyanobacterial
536 light-harvesting mechanisms in glacier cryoconite, *Microbiome*, 10, 1-14,
537 <https://doi.org/10.1186/s40168-022-01238-7>, 2022.



- 538 Musilova, M., Tranter, M., Bamber, J.L., Takeuchi, N. and Anesio, A.M.: Experimental evidence that
539 microbial activity lowers the albedo of glaciers. *Geochem. Perspect. Lett.*, 2, 106-116,
540 <https://doi.org/10.7185/geochemlet.1611>, 2016.
- 541 Nagatsuka, N., Takeuchi, N., Nakano, T., Shin, K. and Kokado, E.: Geographical variations in Sr and
542 Nd isotopic ratios of cryoconite on Asian glaciers, *Environ. Res. Lett.*, 9, 045007,
543 <https://doi.org/10.1088/1748-9326/9/4/045007>, 2014.
- 544 Oksanen, J., Blanchet, F. G., Kindt, R., Legendre, P., O'hara, R., Simpson, G. L., Solymos, P., Stevens,
545 M. H. H., and Wagner, H.: *vegan: Community Ecology Package*. R package version 1.17-2,
546 <https://cran.r-project.org/web/packages/vegan/index.html>, 23, 2010.
- 547 Remias, D., Holzinger, A., Aigner, S. and Lütz, C.: Ecophysiology and ultrastructure of *Ancydonema*
548 *nordenskiöldii* (Zygnematales, Streptophyta), causing brown ice on glaciers in Svalbard (high arctic),
549 *Polar Biol.*, 35, 899-908, <https://doi.org/10.1007/s00300-011-1135-6>, 2012.
- 550 Segawa, T. and Takeuchi, N., Cyanobacterial communities on Qiyi glacier, Qilian Shan, China. *Ann.*
551 *Glaciol.*, 51, 135-144, <https://doi.org/10.3189/172756411795932047>, 2010.
- 552 Segawa, T., Ishii, S., Ohte, N., Akiyoshi, A., Yamada, A., Maruyama, F., Li, Z., Hongoh, Y. and
553 Takeuchi, N.: The nitrogen cycle in cryoconites: naturally occurring nitrification-denitrification
554 granules on a glacier, *Environ. Microbiol.*, 16, 3250-3262, <https://doi.org/10.1111/1462-2920.12543>,
555 2014.
- 556 Segawa, T., Matsuzaki, R., Takeuchi, N., Akiyoshi, A., Navarro, F., Sugiyama, S., Yonezawa, T. and
557 Mori, H.: Bipolar dispersal of red-snow algae, *Nat. Commun.*, 9, 3094,
558 <https://doi.org/10.1038/s41467-018-05521-w>, 2018.
- 559 Segawa, T., Takeuchi, N., Mori, H., Rathnayake, R.M., Li, Z., Akiyoshi, A., Satoh, H. and Ishii, S.,
560 Redox stratification within cryoconite granules influences the nitrogen cycle on glaciers, *FEMS*
561 *Microbiol. Ecol.*, 96, fiae199, <https://doi.org/10.1093/femsec/fiae199>, 2020.
- 562 Segawa, T., Yonezawa, T., Edwards, A., Akiyoshi, A., Tanaka, S., Uetake, J., Irvine-Fynn, T., Fukui,
563 K., Li, Z. and Takeuchi, N.: Biogeography of cryoconite forming cyanobacteria on polar and Asian
564 glaciers, *J. Biogeogr.*, 44, 2849-2861, <https://doi.org/10.1111/jbi.13089>, 2017.
- 565 Segawa, T., Yonezawa, T., Matsuzaki, R., Mori, H., Akiyoshi, A., Navarro, F., Fujita, K., Aizen, V.B.,
566 Li, Z., Mano, S. and Takeuchi, N.: Evolution of snow algae, from cosmopolitans to endemics, revealed



567 by DNA analysis of ancient ice, *ISME J.*, 17, 491-501, <https://doi.org/10.1038/s41396-023-01359-3>,
568 2023.

569 Singh, P., Kumar, N. and Pal, S.: Chapter 10 - Cyanobacteria in the polar regions: diversity, adaptation,
570 and taxonomic problems, *Understanding Present and Past Arctic Environments*, 189-212, ISBN
571 9780128228692, <https://doi.org/10.1016/B978-0-12-822869-2.00013-X>, 2021.

572 Stibal, M. and Tranter, M.: Laboratory investigation of inorganic carbon uptake by cryoconite debris
573 from Werenskioldbreen, Svalbard, *J. Geophys. Res.-Biogeo.*, 112,
574 <https://doi.org/10.1029/2007JG000429>, 2007.

575 Stibal, M., Šabacká, M. and Žárský, J.: Biological processes on glacier and ice sheet surfaces, *Nat.*
576 *Geosci.*, 5, 771-774, <https://doi.org/10.1038/ngeo1611>, 2012a.

577 Stibal, M., Telling, J., Cook, J., Mak, K.M., Hodson, A. and Anesio, A.M.: Environmental controls on
578 microbial abundance and activity on the Greenland ice sheet: a multivariate analysis approach, *Micro.*
579 *Ecol.*, 63, 74-84. <https://doi.org/10.1007/s00248-011-9935-3>, 2012b.

580 Takeuchi, N. and Li, Z.: Characteristics of surface dust on Üürümqi glacier No. 1 in the Tien Shan
581 mountains, China, *Arct. Antarct. Alp. Res.*, 40, 744-750,
582 [https://doi.org/10.1657/1523-0430\(07-094\)\[takeuchi\]2.0.co;2](https://doi.org/10.1657/1523-0430(07-094)[takeuchi]2.0.co;2), 2008.

583 Takeuchi, N., Ishida, Y. and Li, Z.: Microscopic analyses of insoluble particles in an ice core of
584 Üürümqi Glacier No. 1: Quantification of mineral and organic particles, *J. Earth Sci.*, 22, 431-440,
585 <https://doi.org/10.1007/s12583-011-0197-2>, 2011.

586 Takeuchi, N., Sakaki, R., Uetake, J., Nagatsuka, N., Shimada, R., Niwano, M. and Aoki, T.: Temporal
587 variations of cryoconite holes and cryoconite coverage on the ablation ice surface of Qaanaaq Glacier
588 in northwest Greenland, *Ann. Glaciol.*, 59, 21-30, <https://doi.org/10.1017/aog.2018.19>, 2018.

589 Takeuchi, N., Tanaka, S., Konno, Y., Irvine-Fynn, T.D., Rassner, S.M. and Edwards, A.: Variations in
590 phototroph communities on the ablating bare-ice surface of glaciers on Brøggerhalvøya, Svalbard,
591 *Front. Earth Sci.*, 7, 4, <https://doi.org/10.3389/feart.2019.00004>, 2019.

592 Takeuchi, N., Uetake, J., Fujita, K., Aizen, V.B. and Nikitin, S.D.: A snow algal community on Akkem
593 glacier in the Russian Altai mountains, *Ann. Glaciology*, 43, 378-384,
594 <https://doi.org/10.3189/172756406781812113>, 2006.



- 595 Takeuchi, N.: Optical characteristics of cryoconite (surface dust) on glaciers: the relationship between
596 light absorbency and the property of organic matter contained in the cryoconite, *Ann. Glaciology*, 34,
597 409-414, <https://doi.org/10.3189/172756402781817743>, 2002.
- 598 Takeuchi, N.: Seasonal and altitudinal variations in snow algal communities on an Alaskan glacier
599 (Gulkana glacier in the Alaska range), *Environ. Res. Lett.*, 8, 035002,
600 <https://doi.org/10.1088/1748-9326/8/3/035002>, 2013.
- 601 Takeuchi, N.: The altitudinal distribution of snow algae on an Alaska glacier (Gulkana Glacier in the
602 Alaska Range), *Hydrol. Process.*, 15, 3447-3459, <https://doi.org/10.1002/hyp.1040>, 2001.
- 603 Uetake, J., Naganuma, T., Hebsgaard, M.B., Kanda, H. and Kohshima, S.: Communities of algae and
604 cyanobacteria on glaciers in west Greenland, *Polar Sci.*, 4, pp.71-80,
605 <https://doi.org/10.1016/j.polar.2010.03.002>, 2010.
- 606 Uetake, J., Nagatsuka, N., Onuma, Y., Takeuchi, N., Motoyama, H. and Aoki, T.: Bacterial community
607 changes with granule size in cryoconite and their susceptibility to exogenous nutrients on NW
608 Greenland glaciers, *FEMS Microbiol. Ecol.*, 95, fiz075, <https://doi.org/10.1093/femsec/fiz075>, 2019.
- 609 Williamson, C.J., Anesio, A.M., Cook, J., Tedstone, A., Poniecka, E., Holland, A., Fagan, D., Tranter,
610 M. and Yallop, M.L.: Ice algal bloom development on the surface of the Greenland Ice Sheet, *FEMS
611 Microbiol. Ecol.*, 94, fiy025, <https://doi.org/10.1093/femsec/fiy025>, 2018.
- 612 Wu, G., Zhang, C., Li, Z., Zhang, X. and Gao, S.: Iron content and solubility in dust from high-alpine
613 snow along a north-south transect of High Asia, *Tellus B*, 64, 17735,
614 <https://doi.org/10.3402/tellusb.v64i0.17735>, 2012.
- 615 Yallop, M.L., Anesio, A.M., Perkins, R.G., Cook, J., Telling, J., Fagan, D., MacFarlane, J., Stibal, M.,
616 Barker, G., Bellas, C. and Hodson, A.: Photophysiology and albedo-changing potential of the ice algal
617 community on the surface of the Greenland ice sheet, *ISME J.*, 6, 2302-2313,
618 <https://doi.org/10.1038/ismej.2012.107>, 2012.
- 619 Ye, B., Yang, D., Jiao, K., Han, T., Jin, Z., Yang, H. and Li, Z.: The Urumqi River source glacier No. 1,
620 Tianshan, China: changes over the past 45 years, *Geophys. Res. Lett.*, 32,
621 <https://doi.org/10.1029/2005gl024178>, 2005.
- 622 Yoshimura, Y., Kohshima, S. and Ohtani, S.: A community of snow algae on a Himalayan glacier:
623 change of algal biomass and community structure with altitude, *Arct. Antarct. Alp. Res.*, 29, 126-137,
624 <https://doi.org/10.1080/00040851.1997.12003222>, 1997.

<https://doi.org/10.5194/egusphere-2026-1281>

Preprint. Discussion started: 20 March 2026

© Author(s) 2026. CC BY 4.0 License.



625 Yue, X., Li, Z., Li, H., Wang, F. and Jin, S.: Multi-temporal variations in surface albedo on Urumqi
626 glacier No. 1 in Tien Shan, under arid and semi-arid environment, *Remote Sens.*, 14, 808,
627 <https://doi.org/10.3390/rs14040808>, 2022.